NASA TN D-99

TECHNICAL NOTE

D-99

PRINCIPLES OF DESIGN OF DYNAMICALLY SIMILAR

MODELS FOR LARGE PROPELLANT TANKS

By Paul E. Sandorff

Massachusetts Institute of Technology
Cambridge, Massachusetts

NATIONAL AERONAUTICS AND SPACE ADMINISTRATION

WASHINGTON January 1960

NATIONAL AERONAUTICS AND SPACE ADMINISTRATION

TECHNICAL NOTE D-99

PRINCIPLES OF DESIGN OF DYNAMICALLY SIMILAR MODELS FOR LARGE PROPELLANT TANKS

By Paul E. Sandorff*

SUMMARY

A study is made of the similitude conditions existing between a full-scale propellant tank such as would be used for a large rocket vehicle and a dynamically similar, reduced scale model. Scaling laws are derived which permit the design of such a model for a large 40-foot-diameter liquid-oxygen JP-4 tank used as an example. Permutations of different design combinations for the model are examined to determine their suitability and practicability. It is concluded that dynamically similar reduced scale models offer a practical means of studying and developing solutions for large elastic-wall propellant tanks.

INTRODUCTION

Dynamic interaction between the mass of the fluid in rocket propellant tanks and lines and the elastic deformations of the containing structure under the wide-spectrum vibratory forces of the engine is a well-recognized problem (ref. 1). It is often treated by lumped-mass representations with analog computing equipment.

Dynamic effects of propellant sloshing in rigid tanks, coupled with control system dynamics, is of recognized importance to the overall vehicle stability and flutter characteristics (refs. 2 and 3). This problem may place an upper limit on tank size for vehicles having a certain mission, or it may require experimental development of slosh-suppression devices such as baffling, compartmentation, etc. Numerous studies have consequently been made to determine the mode shapes, natural frequencies, and the forces and moments associated with propellant sloshing (refs. 2 through 6, for example) and the effects of damping and baffle design have been investigated both analytically and experimentally (refs. 7 through 11).

---

*Associate Professor of Aeronautics and Astronautics, Massachusetts Institute of Technology, Cambridge, Mass., Consultant to National Aeronautics and Space Administration.

Additional dynamic interaction effects involving elastic tank wall deformations due to surging of the propellant mass under low-frequency accelerations such as maneuvering and control are also receiving attention by some agencies. A simple example of this effect is the surging overload which occurs in a thin-wall rocket tank due to vertical takeoff acceleration, treated in reference 12. Of much greater complexity are dynamic surging effects of an unsymmetrical nature, which may result from angular and lateral accelerations due to gust and control loads. Interaction of fluid sloshing with overall tank bending has been studied analytically in references 13 and 14; interaction with "breathing" modes deserves attention. L

6

To study dynamic effects such as those described above, and to 3
obtain quantitative data which can be used for design, a dynamically 5
similar model may be used. This report deals with the design requirements for such a model, its possibilities and its limitations.

Previous work upon which this report is based was conducted by the author for the Aerojet-General Corporation, Azusa, California, and published as Part II of Report No. 1376 dated 20 December 1957 under Contract AF 33(616)-3767 (ref. 12).

DIMENSIONAL ANALYSIS

In order to establish the basic parameters which govern conditions of similitude for the dynamic model, a dimensional analysis is made. These parameters will be used to design the model and to establish scale factors with which to interpret data taken on the model. Methods used in this section are those of reference 15.

Significant Quantities

External influences.- The tank filled with fluid is considered as a system in inertial space which is subject to an acceleration (ng). The quantity (ng) is a vectorial function that may vary in direction and magnitude along the trajectory; that is, it is a function of time.

In order to specify the function (ng) it is convenient to identify it by an applied concentrated force $\overline{P}$, lb; applied distributed pressure $\overline{p}$, psf; applied moment $\overline{M}$, ft-lb; applied angular velocity and angular acceleration $\dot{\theta}$ and $\ddot{\theta}$; and possibly others. However, these serve only to establish (ng) and need not be considered individually.

Behavior of the shell wall.- The tank walls may be constructed of simple unstiffened plate, stiffened skin, sandwich structure, or thin skin pressurized for stability. Assuming the stiffness properties to be isotropic with respect to dimensions in the plane of the shell, the following load-strain relations express the rigidity of the shell:

$$N_x = \alpha\left(\epsilon_x + \nu\epsilon_y\right) \qquad N_{yz} = \beta_z\gamma_{yz}$$

$$N_y = \alpha\left(\epsilon_y + \nu\epsilon_x\right) \qquad M_{xx} = D\left(w_{xx} + \nu' w_{yy}\right)$$

$$N_{xy} = \beta_{xy}\gamma_{xy} \qquad M_{yy} = D\left(w_{yy} + \nu' w_{xx}\right)$$

$$N_{xz} = \beta_z\gamma_{xz} \qquad M_{xy} = Bw_{xy}$$

L
6
3
5

The notation, illustrated in figures 1 and 2, is largely the same as in reference 16:

N_x normal force per unit width on edges parallel to y-axis, lb/in.

N_{xy} shearing force per unit width, equal on x- and y-edges, lb/in.

M_x bending moment per unit width on edges parallel to y-axis, in-lb/in.

M_{xy} twisting moment per unit width, equal on x- and y-edges, in-lb/in.

ϵ_x extensional strain parallel to x-axis

γ_{xy} in-plane shearing strain; i.e., shear of an element parallel to xy plane

γ_{xz} transverse shearing strain; i.e., shear of an element parallel to xz plane

w transverse displacement of neutral plane of shell wall, $w(x,y,z)$, in.

w_{xx} bending curvature of neutral plane about y-axis, $\partial^2 w/\partial x^2$, in.$^{-1}$

w_{xy} twisting curvature of neutral plane, $\partial^2 w/\partial x\,\partial y$, in.$^{-1}$

α extensional stiffness, lb/in. $\left(\alpha = Et/\left(1 - \nu^2\right)\right.$ for homogeneous plate$\left.\right)$

β_{xy} in-plane shearing stiffness, lb/in. $\left(\beta_{xy} = Gt\right.$ for homogeneous plate$\left.\right)$

β_z transverse shearing stiffness, lb/in. $\left(\beta_z = Gt\right.$ for homogeneous plate$\left.\right)$

D bending stiffness, in-lb $\left(D = Et^3/12(1 - \nu^2)\right.$ for homogeneous plate$\left.\right)$

B torsional stiffness, in-lb (B = D for homogeneous plate)

ν Poisson's ratio

ν' Poisson-type elastic constant indicating coupling between moment about one axis and curvature about the other ($\nu' = \nu$ for homogeneous plate)

E elastic (Young's) modulus in extension, psi

G shear modulus, psi

t thickness, in.

The stiffnesses $\left(\beta_{xy}, \beta_z, D, \text{and } B\right)$ can be determined either analytically or experimentally. These relations govern the elastic behavior of isotropic sandwich structure and isotropic symmetrically stiffened sheet, and therefore permit consideration of a wide variation in shell wall detail to meet overall elastic properties. Orthotropic siffened skin structure can be handled in the same manner, with additional elastic constants to define anisotropy and crosscoupling of elastic deformation processes (refs. 17 and 18).

The advantage of the above representation is that fine detail such as the actual thickness of the wall, dimensions of stiffener detail if a stiffened shell is used, attachments, etc., need not necessarily be duplicated. The overall shell wall extension and bending are the immediate concern in the model test, not extremely local effects such as material rupture or local buckling, because the latter do not interact with the fluid surge until conditions which produce failure are reached.

Rupture is a design consideration, however, and therefore, stress distributions must often be obtained. Stresses, as such, are not recognized as existing in the shell wall in the above load-strain relations which specify only forces N and moments M. Similitude is preserved with respect to N and M, not stress, and to convert from one to the other, the particular section detail (local thickness, etc.) must be used, which will not necessarily be in scale from model to prototype.

Similarly, insofar as unit weight is concerned, the significant parameter for the shell wall is $\rho_w t_w$, slugs per unit of surface area, not of volume, where t_w is an equivalent distributed thickness measurement for the wall structure.

Other structure.- There may be portions of the tank structure, e.g., baffles, which, in deforming elastically, affect the fluid surging in an important manner, and which cannot be treated as thin plates under plane stress. In such cases it is often possible to express significant deformational characteristics in terms of overall section properties, as is done above for thin plate, and establish similitude requirements for the overall stiffness properties. Thus by introducing an acceptable approximation, the requirement of strict geometric similarity in a small scale model, which is usually costly, is avoided. There are many examples of this technique in the literature (refs. 19 and 20, for example). For the present, however, deflections of only the external thin-wall tank structure will be considered.

Behavior of the fluid.- As demonstrated in references 2 through 6, propellant sloshing is governed primarily by the fluid density ρ_f in combination with tank geometry, strength of the gravitational or acceleration field (ng), and the nature of the forcing function. Reference 12, Part I, indicates that fluid compressibility (or the bulk modulus K) may also be important in establishing natural modes and frequencies of dynamic surging. The severity of the sloshing and surging may be significantly affected and controlled by fluid viscosity μ through design of baffles and interior details of the tank.

A fourth property of the fluid, important because it governs cavitation effects, is the vapor pressure. More strictly, it is the difference between the local absolute pressure in the fluid p and the vapor pressure p_v, which must be overcome by inertial forces to produce cavitation. At any point this differential pressure is expressed by

$$\left(p - p_v\right) = p_i + \rho_f(ng)h - p_v$$

where p_i is the absolute pressure on the free surface of the liquid, that is, the internal gaseous pressure in the tank; and h is the liquid height in the direction of the acceleration (ng).

Quantities which ordinarily may be classed as minor include surface tension and wetting forces. Both are influenced by conditions and impurities at the fluid surface and by the adjacent material or gas. Surface tension wavelets and capillary rise effects are usually measured in fractions of an inch; it is assumed that critical dimensions in the model will be at least an order of magnitude larger and that dynamic effects due to these quantities may therefore be neglected.

Other quantities.- Various loads carried by the tank structure may affect the dynamic system through nonlinear structural deflection and stability. One such load is the difference in pressure across the tank wall, given by $(p - p_a)$, where p is the local pressure in the fluid as defined previously, and p_a is the ambient pressure external to the tank, both in absolute units.

The properties of the gas above the fluid may conceivably influence fluid dynamics, particularly with regard to gas entrainment effects. Although generally undesirable, gas entrainment may be a problem in either the prototype or the model. It is omitted from consideration for the present.

L
6
3
5

Overall geometry.- The overall dimensions of the structure and of the tank cavity are of course of major importance, and where the nature of the fluid flow is complex and unknown, any departure from strict geometric similarity would be unwise. It is possible that for some tank studies, a distortion in scale may prove to be desirable in order to obtain a successful model test, as is the case in hydraulic models of the tidal basins in which the depth scale is reduced less than horizontal dimensions so that gravity effects remain of major importance. For the present problem, however, in its present stage of investigation, a scale distortion of length does not seem advisable.

For dimensional analysis purposes a characteristic or reference length L is selected (for example, tank height) and the length l is used to represent any other geometrical dimension that has a significant effect on the dynamic flow-deflection phenomenon.

Internal or dependent effects.- Under this classification are included all of the resultant effects of the surging phenomenon; that is, the loads and strains in the tank walls, the pressure distribution in the fluid, and displacements of both fluid and structure. These quantities are all functions of both spatial coordinates and time.

Summary of significant quantities.- The significant quantities are summarized in convenient form as follows:

	Quantity	Symbol	Dimensions
General:	Characteristic length	L	ft
	Any pertinent length	l	ft
	Any pertinent time interval	T	sec

	Quantity	Symbol	Dimensions
Tank wall:	Extensional stiffness	α	lb/ft
	In-plane shear stiffness	β_{xy}	lb/ft
	Transverse shear stiffness	β_z	lb/ft
	Bending stiffness	D	ft-lb
	Torsional stiffness	B	ft-lb
	Poisson's ratio	ν	-----------
	Bending Poisson-type ratio	ν'	-----------
	Density of tank wall	$\rho_w t_w$	$\text{lb-sec}^2/\text{ft}^3$
Other structure:	Not considered at present		
Fluid:	Density	ρ_f	$\text{lb-sec}^2/\text{ft}^4$
	Bulk modulus	K	lb/ft^2
	Viscosity	μ	lb-sec/ft^2
	Excess local pressure over vapor pressure	$p - p_v$	lb/ft^2
	Surface tension	not considered	
	Wetting forces	not considered	
	Gas entrainment effects	not considered	
Other:	Pressure differential on tank wall	$(p - p_a)$	lb/ft^2
	Gas properties	not considered	
External influences:	Applied linear displacement	$\bar{X}$	ft
	Applied linear acceleration	(ng)	ft/sec^2
	Applied concentrated force	$\bar{P}$	lb
	Applied concentrated moment	$\bar{M}$	ft-lb
	Applied distributed pressure	$\bar{p}$	lb/ft^2
	Applied rotational velocity	$\dot{\theta}$	sec^{-1}
	Applied rotational acceleration	$\ddot{\theta}$	sec^{-2}

L
6
3
5

	Quantity	Symbol	Dimensions
Internal effects or response:	Load in tank wall	N	lb/ft
	Moment in tank wall	M	ft-lb/ft
	Strain in tank wall	ϵ	-----------
	Local displacement, fluid or tank wall	x	ft
	Local velocity of displacement	$\dot{x}$	ft/sec
	Local acceleration	$\ddot{x}$	ft/sec^2
	Local pressure in fluid	p	lb/ft^2

L
6
3
5

Governing Parameters

There are tabulated 16 independent quantities which represent the important properties of the system, plus a group of 7, which are interrelated so that only one may be considered independent, which represent the external influences. The response of the system is identified by 7 dependent or secondary quantities; i.e., internal effects. In standard manner (ref. 15) 7 nondimensional secondary or response parameters and 15 independent primary parameters are derived, which govern the physical nature of the surging phenomenon. These are discussed below.

Model design methods.- The significance of the parametric analysis is that any one of the response parameters π_R may be expressed as a (undetermined) function of all of the independent parameters π_1, π_2, π_3, etc.:

$$\pi_R = \phi(\pi_1, \pi_2, \pi_3, \ . \ . \ .)$$

When comparing what happens in the model to what happens in the original, π_R has the same value in both model and original if π_1, π_2, π_3, . . . also are all unchanged between model and original: i.e., $(\pi_1)_m = (\pi_1)_o$; $(\pi_2)_m = (\pi_2)_o$; etc. This is the condition of similitude.

A first objective of model design is, therefore, to keep the independent parameters unchanged in numerical value between model and original, while allowing the geometrical scale to be reduced. This may be facilitated by a suitable change in the scales of the other basic dimensions in which the phenomenon is measured: in the present case, the dimensions of force and time (or convenient equivalents, such as mass and acceleration). If this becomes impossible, a distortion of the scale of one or more of the parameters may not invalidate the model provided the effect of scale distortion can be evaluated. Reference 15 indicates many examples of this art. A third use of the parametric relations is to establish scale factors: If similitude exists, then $(\pi_1)_m = (\pi_1)_o$. Any of the components of $(\pi_1)_m$ may, therefore, be found in terms of the other components and $(\pi_1)_o$.

Overall geometry.- Geometric requirements are stated by the parameter

$$\frac{l}{L}$$

where l represents any pertinent length measurement for either structure or fluid. To preserve $\left(\frac{l}{L}\right)_m = \left(\frac{l}{L}\right)_o$ means geometric similarity. Simplification of model construction requires justification of the unimportance of whichever dimensions l are ignored.

Dependent or response parameters.- A useful set of secondary parameters formed of the quantities which measure response of the system are

$$\frac{N}{\alpha},\ \frac{ML}{D},\ \epsilon,\ \frac{x}{L},\ \frac{\dot{x}}{\sqrt{(ng)L}},\ \frac{\ddot{x}}{(ng)},\ \frac{p}{\rho_f(ng)L}$$

To predict the loading on the full-scale tank wall on the basis of measured stress in the model, the relationships

$$\frac{N_o}{\alpha_o} = \frac{N_m}{\alpha_m};\ \frac{M_oL_o}{D_o} = \frac{M_mL_m}{D_m}$$

are used; whereupon, $N_o = (\alpha_o/\alpha_m)N_m$, etc. Similarly all other quantities derived from the model test may be interpreted to yield full-scale information. For the strain ϵ, the scale factor is unity.

The fluid motions (as well as structural motions) defined by x, $\dot{x}$, and $\ddot{x}$, are geometrically similar in model and original according to respective dimensions and according to respective time scales; that is, $(x/L)_m$ observed at time T_m in the model will be equal to $(x/L)_o$ found at time T_o in the original. The relation of T_m to T_o is shown below.

Time scale.- The phenomenon studied is a dynamic one, and both input and response are functions which vary with time. In general, the time scales are not the same for model and original, which means that any of the input or response parameters has a value in the model identical with that in the original only at the instant in time which also corresponds: that is, when the time parameters are also identical. A convenient time parameter is

$$\frac{(ng)T^2}{L}$$

Corresponding time intervals in model and original are therefore given by the relation:

$$\frac{T_m}{T_o} = \sqrt{\frac{L_m}{L_o}\,\frac{(ng)_o}{(ng)_m}}$$

This relation also identifies the scale between periods of natural modes. The frequencies applying to the model, for vibratory forcing functions and for observed cyclic response, are related to those of the full-scale structure inversely as the time intervals, or

$$\frac{f_m}{f_o} = \sqrt{\frac{L_o}{L_m}\,\frac{(ng)_m}{(ng)_o}}$$

Structural similarity.- Similitude of the elastic properties of the tank wall is obtained by holding the values of the following parameters unchanged from prototype to model:

$$\frac{D}{\alpha L^2}, \quad \frac{\beta_{xy}}{\alpha}, \quad \frac{\beta_z}{\alpha}, \quad \frac{B}{D}, \quad \nu, \quad \nu'$$

The first of these is an "unlike stiffness ratio;" it relates bending and extensional stiffnesses and governs scale effects in elastic shell structure. For a uniform-thickness isotropic plate, $D/\alpha = t^2/12$ where t is the plate thickness, and for any other type of surface structure (such as sandwich, stiffened skin, etc.) $D/\alpha > t^2/12$. Therefore, the scaling down of a tank wall structure, which at full scale is made of uniform-thickness plate, requires scaling down of the thickness t in a ratio at least as large as the overall size reduction. To make a relatively thick-skinned model, i.e., $t_m/t_o > L_m/L_o$, requires going out of scale on the stiffness ratio $D/\alpha L^2$.

Unfortunately one of the difficulties in constructing reduced scale models of shell structure is the problem of duplicating thin skin to scale, without introducing material properties variations and fabricational effects of serious nature. Because of such practical difficulties it may be advantageous to go out of scale in $D/\alpha L^2$, particularly if bending deformations are not as important to the fluid surging phenomenon as extensional strain, and if buckling possibilities can be evaluated in some other way.

The requirements of keeping β_{xy}/α, β_z/α, B/D, and ν' unchanged are met if uniform-thickness plate is used for both prototype and model.

Fluid similarity.- To obtain similitude of sloshing and fluid flow, values of the following parameters must be preserved:

$$\frac{\mu^2}{\rho_f{}^2 L^3 (ng)}, \quad \frac{K}{\rho_f L (ng)}, \quad \frac{\left(p_i - p_v\right)}{\rho_f L (ng)}$$

These correspond, respectively, to the Reynolds number, the Cauchy number, and a parameter comparing cavitation resistance to inertial effects. The simplified form of the latter given above follows by substituting for the local fluid pressure in the more general form:

$$\frac{\left(p - p_v\right)}{\rho_f L (ng)} = \frac{\left(p_i + \rho_f (ng) h - p_v\right)}{\rho_f L (ng)} = \frac{\left(p_i - p_v\right)}{\rho_f L (ng)} + \frac{h}{L}$$

In a geometrically similar model h/L is unchanged, therefore to specify $\left(p_i - p_v\right)/\rho_f L(ng)$ the same in model as in prototype is sufficient to guarantee similitude of cavitation effects at all points in the fluid mass. Conversely, if cavitation is a problem, geometrical similarity of the tank cavity is required.

The Froude number is of especial significance in fluid wave motions or sloshing and can be expressed by either $\frac{\dot{x}^2}{(ng)L}$ or $\frac{\ddot{x}}{(ng)}$. These ratios have already been presented as independent parameters; that is, in the present case the Froude number expresses the response of the fluid to external accelerative forces.

Force interactions.- Similitude between the interaction effects between forces due to shell extensional stiffness and, respectively, fluid inertia, fluid compressibility, and fluid vapor pressure, the interaction between shell inertia and fluid inertia, and between cavity pressure and structural rigidity, are governed by:

$$\frac{\rho_f L^2 (ng)}{\alpha}, \quad \frac{KL}{\alpha}, \quad \frac{\left(p_i - p_v\right)L}{\alpha}, \quad \frac{\rho_f L}{\left(\rho_w t_w\right)}, \quad \frac{\left(p_i - p_a\right)L^3}{D}$$

The second and third of these duplicate previous parameters, since they can be formed by combination of the first with the parameters $\frac{K}{\rho_f L(ng)}$ and $\frac{(p_i - p_v)}{\rho_f L(ng)}$ of the previous section.

The ratio of fluid mass to structural mass $\rho_f L/\rho_w t_w$ is ordinarily unimportant because of the small deflection and small mass of the structure. The parameter $(p_i - p_a)L^3/D$ governs the effects of internal L
pressure on shell stability, and may be derived from the more general 6
relation which is written in terms of the local pressure differential 3
$(p - p_a)$: 5

$$\frac{(p - p_a)L^3}{D} = \frac{(p_i - p_a)L^3}{D} + \frac{\rho_f(ng)hL^3}{D}$$

The second term of the above when combined with the parameters $\rho_f L^2(ng)/\alpha$ and $D/\alpha L^2$ yields h/L, which is constant for geometric similarity; consequently the first term suffices if similitude holds for geometry, structure and fluid mechanics. By the same combination the alternate form $(p_i - p_a)/\rho_f L(ng)$ may be shown.

The parameter $\rho_f L^2(ng)/\alpha$ (or its alternate $\rho_f L^4(ng)/D$) is by far the most important in determining dynamic interaction effects in fluid surging in thin-wall tanks. The denominator of this parameter represents the force due to elastic characteristics of the tank, to an accuracy determined by the excellence to which complete structural similarity is obtained, while the numerator is a measure of the fluid surging input force.

External influences.- In the parameters presented above the externally applied acceleration, (ng), has been treated as a prime quantity defining the behavior of the system. Indeed it may be considered as a basic dimension, and it is explicitly under the control of the experimentalist by his selection of amplitude versus time program of the applied disturbance. Various types of applied external loading are related to the resultant acceleration (ng) in manner such as to maintain the following parameters unchanged in value between model and original:

$$\frac{\bar{X}}{(ng)t^2}, \quad \frac{\bar{P}}{\rho_f L^3(ng)}, \quad \frac{\bar{M}}{\rho_f L^2(ng)}, \quad \frac{\bar{p}}{\rho_f L(ng)}, \quad \frac{\dot{\theta}^2 L}{(ng)}, \quad \frac{\ddot{\theta} L}{(ng)}$$

Any one of these may alternatively be taken as a statement of Newton's law of motion. If, in setting up for the dimensional analysis problem, density were accorded the dimensions of mass, the external influences $\bar{X}$, $\bar{P}$, etc. would necessarily be expressed only in terms of each other and one less parameter would appear above. It is more convenient, however, to retain the acceleration (ng) as a variable which may be manipulated by the designer. The extra parameter describes a test condition which must be met in any case, whether for similitude or in accordance with Newton's law.

MODEL DESIGN

The requirements developed in the preceding section are here applied to derive a suitable design for a small-scale model of a propellant tank. The properties of the tank structure and propellants to be simulated are identified in figure 3.

Preliminary Model Design Considerations

Length scale.- Three factors influence the selection of the scale of the model:

(a) Convenience of establishing test conditions and loads

(b) Fabricational cost

(c) Accuracy of quantitative data

An optimum size exists for each of these, which varies with the design and the program. However, consideration of (a) would indicate a maximum model size of perhaps 15 feet overall length, while consideration of (c) would establish the minimum practicable length of perhaps 3 feet overall. Therefore to investigate the effects of model design considerations, scale reductions of 1/8 and 1/16 are studied.

Loading.- Five types of loading programs are considered:

(a) Thrust simulation, in which (ng) is directed always axially and increases from $n = 1$ to $n = 1 + (\Delta n)_{takeoff}$ in accordance with thrust buildup at starting, then increases slowly as propellant is consumed, and finally is reduced to zero according to engine cutoff characteristics.

(b) Maneuvering, in which (ng) is essentially constant in magnitude but varies in direction through control of rocket thrust vector.

(c) Vibrational accelerations due to engine operation.

(d) Airload, in which a lateral component of (ng) is brought about by external pressure distribution on the tank wall.

(e) Portions or combinations of the above.

Simulation of all of these conditions simultaneously does not appear practicable. A "slosh table" apparatus, however, has been used with considerable success in the study of propellant sloshing in rigid
tanks (refs. 7, 11). In this case longitudinal acceleration, which L
may be any value of the thrust/weight ratio that occurs in flight, is 6
simulated by normal gravity in the model, and a cyclic heaving transla- 3
tion of low amplitude is introduced to evaluate frequency response and 5
damping of the partially full tank. This same type of apparatus could be applied for the study of unsymmetrical modes involving structural deformations.

In the case of vibration testing, the cyclic disturbing force is applied longitudinally and represents vibratory variations in normal engine thrust. Conducted under normal gravity, the model test has the same acceleration scale as the slosh table test.

In addition to such basic research, it may be desirable to investigate coupling effects between various modes and systems for specific designs. For this purpose the slosh table might consist of a lightweight roller support and a thrusting armature, controlled by sensors mounted on the tank and a feedback loop whose dynamic characteristics approximate, in the time scale of the model, the control system of the vehicle. If the model is supported at the engine mount gimbal, with some freedom to pitch about an axis transverse to the actuator, flight stability in one plane would be dynamically represented. Anticipated aerodynamic disturbing forces and moments could then be applied according to a selected program and the complex interrelationships of structural modes, fluid flow, and control-system dynamics could be quantitatively studied.

The possibility of symmetrical surging in large rockets is fortunately confined to thrust initiation and cutoff, so that coupling with transverse phenomena need not be considered. To simulate longitudinal variations in acceleration, a centrifuge could be employed; however, spurious tangential and pitching accelerations would be introduced which would be unacceptably large when simulating conventional rocket behavior on practical-sized equipment. Alternatively, a linear acceleration table could be constructed, using either an elevator drive or a rocket sled on, typically, a vertical track 20 or 30 feet high. Design for a dynamically similar test of this type contrasts strongly with that for the slosh table, because it is possible (although not necessary) to use a much higher acceleration scale.

From these considerations two different acceleration scale factors are selected for study:

(a) Minimum (slosh table): $(ng)_m / (ng)_o = 0.2$

(b) Maximum (vertical accelerator): $(ng)_m / (ng)_o = 2.0$

Fluid properties.- A partial list of the physical properties of various propellants and fluids which might be considered for model test purposes is presented in table 1. Excluding exotic materials and extreme conditions, the following represent a range in characteristics and are therefore studied further for suitability in the present test:

L
6
3
5

(a) Liquid oxygen and JP-4, to be used in the model exactly as in the full-scale tank

(b) Water, because of availability and ease of handling

(c) Mercury, because of its extreme density and low viscosity; disadvantages are cost, opacity, and alloying activity with some metals

(d) Methylene chloride, which has a moderately high compressibility and vapor pressure along with a good density-viscosity ratio. An organic solvent, it cannot be used with most plastics.

Other model fluids might be selected for their specific properties; in ref. 7, for example, viscous effects in kerosene were simulated with a 1/7-scale model using methylene bromide. Some latitude in fluid properties may be obtained through the use of mixtures and control of test temperature.

Tank structure.- For practical reasons, materials considered suitable for model construction are limited to those for which fabrication, forming, and joining techniques are simple and well established. The material must be uniform and homogeneous on a scale which is small compared to the size of the expected stress field. Strength considerations must be included in the model design to insure against failure during a vigorous dynamic test program. A structural test may also be envisioned. Transparency would be an attribute. From these general considerations, four different materials are selected which represent the range of properties available. These are described in table 2 and below:

(a) Transparent material: Plexiglas II is a craze-resistant type of methyl methacrylate plastic sheeting manufactured by Rohm and Haas Corp. and used extensively for aircraft cockpit enclosures. It can be obtained on special order in any thickness; it is readily formed and fabricated; and it has good structural properties at room temperature and also at very low temperature. Special forming and cementing techniques must be used to minimize crazing tendencies during subsequent use.

(b) Low-modulus material: Plastic-impregnated fiberglas mat may be low-pressure molded into sheet or into final finished contours using any of several resins. "Void-free" sheeting has a degree of transparency. Adhesive bonding is conventional. Impregnate made of fiberglas cloth is specifically not included here because of its anisotropy and Poisson ratio effects, which make it unattractive for modeling isotropic metallic sheet.

L
6
3
5

(c) Aluminum alloy: Included in this category are rolled sheet products such as 2024-T4 and 7075-T6 alloys, which are commercially available in thicknesses down to 0.010 and 0.012 inch, and may be reduced to as little as a few thousandths by the process of chemical milling. Alloys such as 3S-1/2H and 25S-1/2H which may be available in foil thicknesses have substantially the same elastic properties but considerably lower strength. Assembly would probably use adhesive bonded lap joints, which must be carefully designed to avoid serious local stiffness distortions in the model.

(d) Steels: Stainless steel of the 18-8 variety can be obtained in cold-worked sheet stock as thin as 0.002 inch with tensile ultimate strength values above 200,000 psi. Forming of such stock to fabricate doubly-contoured parts would probably involve developmental work and might result in lower tensile strengths. Electrolytically deposited nickel has been suggested as a material for fabricating complete shells of thickness of the order of 0.002 to 0.005 inch, but with only moderate strength properties. Several other fabricational possibilities in ferrous materials would produce similar elastic and strength properties. Ordinary alloy steels may be considered in the event that the fluid used in the tests does not require low temperature.

Possible Design Combinations

Suitability of fluids for various designs.- The four independent parameters governing fluid flow similitude are all formed in terms of ρ_f, L, and (ng), the three dimensions over which the designer has freedom of choice. This makes it possible to consider permutations over the selected practical ranges of length, density, and acceleration scales and to determine what the requirements in fluid properties are for each combination. This has been done in table 3 for the viscous and compressibility effects, and the absolute pressures required inside and outside of the tank have been computed for each case using the relations

$$\left(p_i\right)_m = \frac{\Delta p_m}{\Delta p_o}\left(p_i - p_v\right)_o + \left(p_v\right)_m$$

$$\left(p_a\right)_m = \left(p_i\right)_m - \frac{\Delta p_m}{\Delta p_o}\left(p_i - p_a\right)_o$$

assuming $\left(p_a\right)_o = 14.7$ psia and $\left(p_i\right)_o = 75$ psia. Comparison with the available properties of table 1 leads to the following conclusions:

(a) Viscous forces in all cases considered are disproportionately greater in the model than in full scale. Mercury as a model fluid has the most favorable properties, but for the 1/8-scale slosh test, even this fluid has a viscosity-density ratio six times too large to simulate the behavior of JP-4, thirty times too large to simulate liquid oxygen.

Although some improvement might be expected through more careful selection of fluid and control of test conditions, going out of scale on viscous damping effects appears unavoidable. One approach would require a series of tests on models of different size, or under different scales of acceleration or with different fluids, so that the scale effect for viscous damping could be evaluated, permitting extrapolation of the test data to predict full-scale performance.

Presuming that some form of baffling would be necessary, a more sophisticated method would attempt to scale the slosh damping forces rather than the fluid viscosity. This approach would lead to baffle detail design for the model which is less efficient than for the full-scale structure, to compensate for the viscosity effect; for example, size of perforations in a baffle plate may not be reduced to scale. Additional tests may also be necessary in this case.

(b) In all cases considered, the fluid used in the model has insufficient compressibility (too rigid, K_m too large) to achieve similitude. The best approximation, of the order of 1/4, is obtained with a 1/8-scale model at an acceleration scale of 2 times the original.

None of the common fluids of table 1, including the silicones often used for liquid springs, is sufficiently compressible to meet the needs; liquid hydrogen is excepted because of complications which it would introduce into the conduct of the test. Some artificial means may be employed, however, such as the use of many small gas capsules, as illustrated in figure 4, distributed uniformly throughout the volume. This scheme has the disadvantage, in addition to complexity and cost, of producing local flow inaccuracies and increasing apparent viscosity. But with it similitude in one important respect can be achieved using any fluid which might prove desirable from other considerations.

(c) Vapor pressure effects insofar as they may influence cavitation in the surging propellant can be simulated in the model with any test fluid by adjusting the internal gas pressure in the tank cavity. However, the pressures required are in many cases extreme, and when considered simultaneously with the problem of simulating the proper pressure differential across the tank wall for structural stability, it is seen that an enclosing pressure vessel would be necessary to furnish control of the ambient pressure external to the test tank, in some instances down to a complete vacuum.

L
6
3
5

In almost all cases, if the ambient pressure is atmospheric and the internal cavity pressure is adjusted to the correct value for structural stability, the model will be unconservative in reproducing cavitation effects. If such phenomena are considered serious a suitable test could be achieved by using a model fluid such as methylene chloride at an elevated temperature.

The use of mercury can be particularly disadvantageous in models for which the scale reduction is not large, because extremely high tank pressures are necessary to prevent unwanted cavitation effects.

Tank strength considerations.- Assuming similitude is achieved in the model, the margin of safety in static strength in various model designs can be compared with that which applies to the full-scale structure. If the critical running load which produces failure of the full-scale tank is $\left(N_u\right)_o$ lb/in, then the local stress at failure is

$$\left(f_{ty}\right)_o = \frac{\left(K_t\right)_o\left(N_u\right)_o}{t_o}$$

where $\left(K_t\right)_o$ is a stress concentration factor. The margin of safety, MS, based on tensile yield F_{ty} as allowable, is then given by

$$(MS)_o = \frac{\left(F_{ty}\right)_o}{\left(f_{ty}\right)_o} - 1 = \frac{\left(F_{ty}\right)_o t_o}{\left(K_t\right)_o\left(N_u\right)_o} - 1$$

For the model a similar relation may be written:

$$(MS)_m = \frac{\left(F_{ty}\right)_m}{\left(f_{ty}\right)_m} - 1 = \frac{\left(F_{ty}\right)_m t_m}{\left(K_t\right)_m\left(N_u\right)_m} - 1$$

Comparing the two MS relations gives:

$$\frac{\left(1 + (MS)_m\right)}{\left(1 + (MS)_o\right)} = \frac{\left(K_t\right)_o}{\left(K_t\right)_m} \frac{\left(F_{ty}\right)_m}{\left(F_{ty}\right)_o} \frac{\left(N_u\right)_o}{\left(N_u\right)_m} \frac{t_m}{t_o}$$

Dynamic similitude of extensional stiffness (assumed to be preserved) means that $\left(N_u\right)_m / \left(N_u\right)_o = \alpha_m/\alpha_o$. By substitution and rearrangement, a figure of merit φ, which applies when other properties are held so as to achieve similitude, is defined as

$$\begin{aligned}
\varphi &= \left[\frac{\left(1 + (MS)_m\right)}{\left(1 + (MS)_o\right)} \frac{\left(K_t\right)_m}{\left(K_t\right)_o}\right] \\
&= \left[\frac{\left(F_{ty}\right)_m}{\left(F_{ty}\right)_o} \frac{\alpha_o}{\alpha_m} \frac{t_m}{t_o}\right] \\
&= \left[\frac{\left(F_{ty}\right)_m}{\left(F_{ty}\right)_o} \frac{E_o / \left(1 - \nu_o^2\right)}{E_m / \left(1 - \nu_m^2\right)}\right]
\end{aligned}$$

The quantity φ is a measure of the suitability of any material from a strength viewpoint, as compared with the material used in the full-scale structure. Stress concentration effects may, of course, vary from the original to the model. However, if φ is much greater than unity, then a considerable latitude is permissible in model fabrication and a rugged model is assured, while if φ is less than unity, much care must be exercised both in the construction of the model and also in its use. Values of φ for the several different materials considered in this study are computed in table 2.

It is clear that a dynamically similar model cannot be constructed of Plexiglas II without going submarginal in strength. Fiberglas impregnate, however, offers a comfortable margin of safety and would therefore be advantageous for model construction. Dynamically similar models in aluminum alloy, or steel, would also be approximately similar in strength.

Tank-wall rigidity considerations.- In table 4 the four model constructional materials previously described are studied for use in the 1/8-scale models, with water and mercury as the model fluids, assuming use of a uniform-thickness isotropic sheet for the model as well as for the full-scale tank. The ratio of skin thicknesses to meet the required extensional stiffness, so that $\rho_f L^2 (ng) / \alpha$ is preserved, is first found for each model design. Then the scale of the unlike-stiffness parameter $D/\alpha L^2$ is computed assuming uniform-thickness sheet. For proper duplication of the bending and buckling effects in the model, $\left(D/\alpha L^2\right)_m / \left(D/\alpha L^2\right)_o$ should be unity.

The use of mercury as a model fluid, it is seen, requires tank-wall thicknesses for proper stiffness which, for Plexiglas and fiber-glas construction, would be somewhat extreme. From the value of φ in table 2, strength considerations would not alter this qualitative
appraisal, although the pressures which must be carried by these tanks, L
from table 3, are decidedly unattractive. For a model of aluminum 6
alloy or steel, however, mercury leads to thicknesses which would be 3
advantageous from a fabrication standpoint. 5

Even with a low-density fluid, the use of Plexiglas requires tank walls which are too stiff in bending to furnish similitude in $D/\alpha L^2$. For most other cases, however, the wall thickness is reduced in a greater ratio than the overall dimensions, and local bending stiffness consequently is too low in the model. This condition can be corrected by the use of a close pattern of uniformly spaced stiffening elements in the model wall. An isotropic design which will give the proper increase in D_m without affecting α_m could be achieved in aluminum alloy or steel through the use of chemical milling. Adhesive bonding of a grid of rectangular stiffeners could also be employed.

Introducing such detail into the model structure would produce dissimilarity in the in-plane shear stiffness β_{xy}. Shear stiffness terms would ordinarily be of minor importance compared to $D/\alpha L^2$. The variations in ν between different materials considered, and possible variations in ν' between different detail designs, are also of secondary importance.

CONCLUSIONS

It appears feasible and practical to study the dynamic behavior of large rocket propellant tanks through the use of reduced scale models. The most difficult aspect of such dynamically similar model tests is the proper simulation of viscous effects. If the original propellant is viscid, any one of many suitable low viscosity fluids can be used to permit a reduction in size. But common rocket propellants have low viscosity-to-density ratios; that for liquid oxygen, for example, is lower than that of any of the common fluids which might be suggested for use in the model. In such cases, if any worthwhile reduction in size is to be made in the test model, it appears that viscous damping effects will be disproportionately large. Viscous effects are of major importance in the study of methods for control of propellant sloshing, and correction for scale effects must be made. An extended test program varying one of the "dimensions" of the model may be necessary to evaluate the scale effect in sloshing; or alternatively, it may be possible to represent full-scale effects in the model by variation in the detail design of the baffle structure.

Other important properties of the fluid include compressibility and vapor-pressure effects. In the reduced scale model the fluid is generally too incompressible, and the vapor pressure is generally too low for similitude. Some practical methods of correcting these shortcomings, for limited test purposes, are suggested.

Proper rigidity of the model tank structure to achieve dynamic similitude of the interaction with fluid flow appears to be available with a number of constructional materials. Of these, fiberglas mat impregnate has the advantage, in the case studied, of furnishing a higher margin of safety on strength than would be true of the full-scale steel structure.

Massachusetts Institute of Technology,
Cambridge, Massachusetts.

REFERENCES

1. Ashley, H.: Dynamic Effects of Fuel in Tanks. Section XI of Notes for a Special Summer Session in Aerodynamics of Missiles, MIT, June 1957.

2. Lorell, Jack: Forces Produced by Fuel Oscillations. Progress Rep. No. 20-149 (Contract No. DA-04-495-Ord 18), C.I.T., Jet Propulsion Lab., Oct. 16, 1951.

3. Graham, E. W., and Rodriguez, A. M.: The Characteristics of Fuel Motion Which Affect Airplane Dynamics. Rep. No. SM-14212, Douglas Aircraft Co., Inc., Nov. 27, 1951.

4. Kachigan, K.: Forced Oscillations of a Fluid in a Cylindrical Tank. Rep. ZU-7-046 (Contract No. AF04(645)-4), CONVAIR, Oct. 4, 1955.

5. Bauer, Helmut F.: Fluid Oscillations in a Circular Cylindrical Tank. Rep. No. DA-TR-1-58, Dev. Operations Div., Army Ballistic Missile Agency (Redstone Arsenal, Ala.), Apr. 1958.

6. Lawrence, H. R., Wang, C. J., and Reddy, R. B.: Variational Solution of Fuel Sloshing Modes. Jet Propulsion, vol. 28, no. 11, Nov. 1958, pp. 729-736.

7. Bauer, Helmut F.: Fluid Oscillation in a Cylindrical Tank With Damping. Rep. No. DA-TR-4-58, Dev. Operations Div., Army Ballistic Missile Agency (Redstone Arsenal, Ala.), Apr. 1958.

8. Miles, J. W.: Ring Damping of Free Surface Oscillations in a Circular Tank. Jour. Appl. Mech., vol. 25, no. 2, p. 274, June 1958.

9. Eulitz, Werner: A Can-Type Anti-Slosh Device Derived From Basic Slosh Studies. Rep. DSD-TR-4-58, Dev. Operations Div., Army Ballistic Missile Agency (Redstone Arsenal, Ala.), Aug. 1958.

10. Abramson, H. N., and Ransleben, G. E., Jr.: A Theoretical and Experimental Study of Fuel Sloshing. Southwest Research Institute Progress Rep. No. 13 (Contract No. DA-23-072-ORD-1251), May 1, 1959.

11. Abramson, H. N., and Ransleben, G. E., Jr.: Simulation of Fuel Sloshing Characteristics in Missile Tanks by Use of Small Models. Southwest Res. Inst. Tech. Rep. No. 3 (Contract DA-23-072-ORD-1251), March 20, 1959.

12. Sandorff, P. E., and Petersen, L. K.: Propellant Tank Dynamics. Aerojet-General Corp. Rep. No. 1376 (Contract AF33(616)-3767), December 20, 1957.

13. Bauer, Helmut F.: Damped Fluid Oscillations in a Circular Cylindrical Tank Due to Bending of Tank Wall. Rep. No. DA-TR-9-58, Dev. Operations Div., Army Ballistic Missile Agency (Redstone Arsenal, Ala.), May 1958.

14. Miles, J. W.: On the Sloshing of Liquid in a Flexible Tank. Jour. Appl. Mech., vol. 25, no. 2, p. 277, June 1958.

15. Murphy, Glenn: Similitude in Engineering. The Ronald Press Co., 1950.

16. Timoshenko, S.: Theory of Elastic Stability. McGraw-Hill Book Co., Inc., 1936.

17. Crawford, Robert F.: A Theory for the Elastic Deflections of Plates Integrally Stiffened on One Side. NACA TN 3646, 1956.

18. Libove, Charles, and Hubka, Ralph E.: Elastic Constants for Corrugated-Core Sandwich Plates. NACA TN 2289, 1951.

19. Loudenslager, O. W.: Structural Model Testing. SAE Jour. (Trans.), vol. 54, no. 1, Jan. 1946, pp. 18-25.

20. Raphael, Coleman: Considerations in the Design of Structural Models. Aero. Eng. Rev., vol. 14, no. 2, Feb 1955, pp. 52-55.

21. Div. Chem. Eng.: Liquid Propellants Handbook. Contract NOa(s) 54-597-c, Battelle Memorial Inst., Oct. 19, 1956.

22. Hodgman, Charles D., ed.: Handbook of Chemistry and Physics. Thirty-sixth ed., Chemical Rubber Pub. Co., 1954-1955.

23. Lange, Norbert Adolph: Handbook of Chemistry. Eighth ed., Handbook Publishers, Inc. (Sandusky, Ohio), 1952.

24. Schaafs. W.: Untersuchungen uber Schallgeschwindigkeit und Konstitution, I, Die Schallgeschwindigkeit in organischen Flussigkeiten. Zeitschrift fur physikalische Chemie, vol. 194, p. 34, 1944.

TABLE 1.- PHYSICAL PROPERTIES OF VARIOUS PROPELLANTS AND FLUIDS

		Density	Compressibility		Viscosity, μ, poises (a)	Surface tension, γ, $\frac{dynes}{cm}$ (b)	Vapor pressure, p_v, lb/sq in. abs.	Reference
		ρ_f specific gravity	$\beta = -\frac{\Delta V}{V \Delta p}$ unit vols. per atmos.	$K = V \frac{\Delta p}{\Delta V}$ lb/ft^2 per unit vol.				
Acetone	68° F	0.79	120×10^{-6}	18×10^{6}	0.0033	23	3.58	23
Ammonia, liq.	-28° F	.68	75	28	.0026	34	14.7	21
Analine	68° F	1.02	37	57	.044	44	.005	21
Benzene	68° F	.90	95	22	.0065	29	1.54	23
Ethyl ether	68° F	.74	165	13	.0023	17	8.53	23
Ethyl alcohol	68° F	.79	112	19	.012	22	.85	21
Fluorine, liq.	-306° F	1.54	-------------	---------	.0035	10	14.7	21
Glycerine	68° F	1.261	22	96	14.99	63	---------	23
Hydrazine N_2H_4	68° F	1.009	23	92	.0097	75	.020	21
Hydrogen, liq.	-439° F	.071	19,200	0.11	.00013	1.9	14.7	22
Hyd. peroxide H_2O_2	68° F	1.44	-------------	---------	.0125	76	.027	21
JP-4	68° F	.78	85	25	.0083	-----	---------	21
Methyl alcohol	68° F	.81	120	18	.0059	22	1.85	23
Methylene chloride CH_2Cl_2	68° F	1.34	64	33	.0044	27	6.7	22, 23, 24
Mercury	68° F	13.56	3.9	540	.016	476	.000023	23
Octane C_8H_{18}	68° F	.72	121	18	.0054	22	.19	21, 22, 23
Oxygen, liq.	-297° F	1.14	106	20	.0019	13	14.7	21
Red fum, nitric acid	68° F	1.56	-------------	---------	.014	-----	2.05	21
Silicone No. 200, 0.65 c.s.	68° F	.76	180	12	.005	-----	---------	Manufacturer's data
(Dow-Corning) 3.0 c.s.	68° F	.90	180	12	.028	-----	---------	Manufacturer's data
UDMH	68° F	.79	-------------	---------	.0051	28	2.37	21
Wh. fum. nitric acid	68° F	1.51	47	45	.0086	41	.93	21
Water	68° F	.998	49.1	43	.010	73	.34	22, 23

[a]To convert poises to lb-sec/ft^2 multiply by 2.089×10^{-3}.

[b]To convert dynes/cm to lb/ft multiply by 6.853×10^{-5}.

TABLE 2.- STRUCTURAL PROPERTIES OF SOME SELECTED TANK WALL MATERIALS

[Approximate room-temperature properties]

Material	Modulus of elasticity, E, psi	Poissons ratio, ν	$\frac{E}{1 - \nu^2}$, psi	Density, ρ_w, lb/in^3	Allowable tensile yield stress, F_{ty}, psi	Figure of merit, φ (a)
Plexiglas II	0.4×10^6	0.35	0.45×10^6	0.043	[b]1,500	0.53
Fiberglas mat impregnate	1.2×10^6	.35	1.37×10^6	.055	15,000	1.74
Aluminum alloy 7075-T6	10.5×10^6	.33	11.2×10^6	.10	68,000	.97
Stainless steel 302-FH	29×10^6	.30	32.0×10^6	.29	200,000	1.00

[a]Value of $\varphi > 1.0$ for the model material indicates a margin of safety for the model better than that for the full-scale structure. Based on use of stainless steel for the full-scale tank.

[b]Probable maximum to avoid crazing in repeated use.

L
6
3
5

1Z

TABLE 3.- REQUIRED FLUID PROPERTIES AND PRESSURES FOR SIMILITUDE WHEN ASSUMING CERTAIN PRACTICAL COMBINATIONS OF LENGTH, ACCELERATION, AND MODEL FLUID

Selected variations					Viscosity effects		Compressibility and pressure effects			
Length scale, L_m/L_o	Acceleration scale, $(ng)_m/(ng)_o$	Model fluid	Original fluid	Fluid-density scale, $(\rho_f)_m/(\rho_f)_o$	$\frac{\mu_m}{\mu_o} = \sqrt{\frac{\left[\rho_f{}^2L^3(ng)\right]_m}{\left[\rho_f{}^2L^3(ng)\right]_o}}$	$\frac{\mu_{m,req}}{\mu_{m,act}}$	$\frac{K_m}{K_o} = \frac{\Delta p_m}{\Delta p_o} = \frac{\left[\rho_f L(ng)\right]_m}{\left[\rho_f L(ng)\right]_o}$	$\frac{K_{m,req}}{K_{m,act}}$	Required internal pressure, $(p_i)_m$, psia	Required ambient pressure, $(p_a)_m$, psia
1/8	1/5 (slosh table)	lox	lox	1.0	0.020	0.020	0.025	0.025	16.2	14.7
		JP-4	JP-4	1.0	.020	.020	.025	.025	2.08	.58
		Water	lox	.88	.017	.003	.022	.010	1.66	.34
		Water	JP-4	1.28	.025	.021	.032	.018	2.74	.82
		Mercury	lox	11.9	.24	.029	.30	.011	18.0	.00
		Mercury	JP-4	17.4	.34	.17	.40	.020	33.0	6.6
		Methylene-chloride	lox	1.16	.023	.01	.029	.018	8.4	6.7
			JP-4	1.69	.033	.06	.042	.032	9.8	7.3
	2.0 (vertical acceleration)	lox	lox	1.0	0.063	0.063	0.25	0.25	30.0	14.7
		JP-4	JP-4	1.0	.063	.063	.25	.25	19.0	4.0
		Water	lox	.88	.055	.010	.22	.10	13.5	.3
		Water	JP-4	1.28	.080	.066	.32	.19	24.3	5.1
		Mercury	lox	11.9	.74	.088	3.0	.11	180.0	.00
		Mercury	JP-4	17.4	1.09	.57	4.4	.20	330.0	66.0
		Methylene-chloride	lox	1.16	.072	.03	.29	.18	24.1	6.7
			JP-4	1.69	.106	.20	.42	.32	38.2	13.0
1/16	1/5	lox	lox	1.0	0.007	0.007	0.012	0.012	15.5	14.7
		JP-4	JP-4	1.0	.007	.007	.012	.012	1.1	.4
		Water	lox	.88	.006	.001	.011	.005	1.0	.3
		Water	JP-4	1.28	.009	.007	.016	.009	1.5	.6
		Mercury	lox	11.9	.083	.010	.15	.006	9.0	.00
		Mercury	JP-4	17.4	.121	.063	.22	.010	16.5	3.3
		Methylene-chloride	lox	1.16	.008	.003	.014	.009	7.6	6.7
			JP-4	1.69	.012	.023	.021	.016	8.3	7.0
	2.0	lox	lox	1.0	0.022	0.022	0.12	0.12	22.2	14.7
		JP-4	JP-4	1.0	.022	.022	.12	.12	9.6	2.1
		Water	lox	.88	.019	.004	.11	.05	7.0	.3
		Water	JP-4	1.28	.028	.023	.16	.09	12.3	2.7
		Mercury	lox	11.9	.26	.031	1.5	.06	90.0	.00
		Mercury	JP-4	17.4	.38	.20	2.2	.10	165.0	33.0
		Methylene-chloride	lox	1.16	.026	.011	.14	.09	15.4	6.7
			JP-4	1.69	.037	.07	.21	.16	22.5	9.9

Vapor pressure of JP-4 taken as 0.20 lb/in.^{2}. Other properties from table 1.

TABLE 4.- MODEL WALL THICKNESS FOR PROPER EXTENSIONAL STIFFNESS AND THE RESULTANT SCALE OF BENDING STIFFNESS (ASSUMING UNIFORM-THICKNESS PLATE FOR BOTH MODEL AND ORIGINAL)

$\frac{L_m}{L_o}$	$\frac{(ng)_m}{(ng)_o}$	Model fluid	Original fluid	$\frac{(\rho_f)_m}{(\rho_f)_o}$	$\frac{\alpha_m}{\alpha_o} = \frac{\left[\rho_f L^2(ng)\right]_m}{\left[\rho_f L^2(ng)\right]_o}$	Model material	Thickness ratio for proper extensional stiffness, $\frac{t_m}{t_o} = \frac{E_o/(1 - \nu_o^2)\alpha_o}{E_m/(1 - \nu_m^2)\alpha_m}$	Resultant ratio of bending stiffnesses, $\frac{(D/\alpha L^2)_m}{(D/\alpha L^2)_o} = \left(\frac{t_m/t_o}{L_m/L_o}\right)^2$
1/8	1/5	Water	lox	0.88	0.0028	Plexiglas II	0.200	2.5
						Fiberglas impregnated	.065	.272
						Aluminum alloy	.0080	.0041
						Stainless steel	.0028	.0005
			JP-4	1.28	.0040	Plexiglas II	.284	5.2
						Fiberglas	.093	.55
						Aluminum alloy	.0114	.008
						Stainless steel	.0040	.001
		Mercury	lox	11.9	0.037	Plexiglas II	2.6	430
						Fiberglas	.86	47
						Aluminum alloy	.11	.78
						Stainless steel	.037	.09
			JP-4	17.4	.054	Plexiglas II	3.8	920
						Fiberglas	1.26	101
						Aluminum alloy	.154	1.5
						Stainless steel	.054	.19
1/8	2	Water	lox	0.88	0.028	Plexiglas II	2.00	253
						Fiberglas	.65	27
						Aluminum alloy	.080	.41
						Stainless steel	.028	.05
			JP-4	1.28	.040	Plexiglas II	2.84	515
						Fiberglas	.93	55
						Aluminum alloy	.11	.78
						Stainless steel	.04	.10

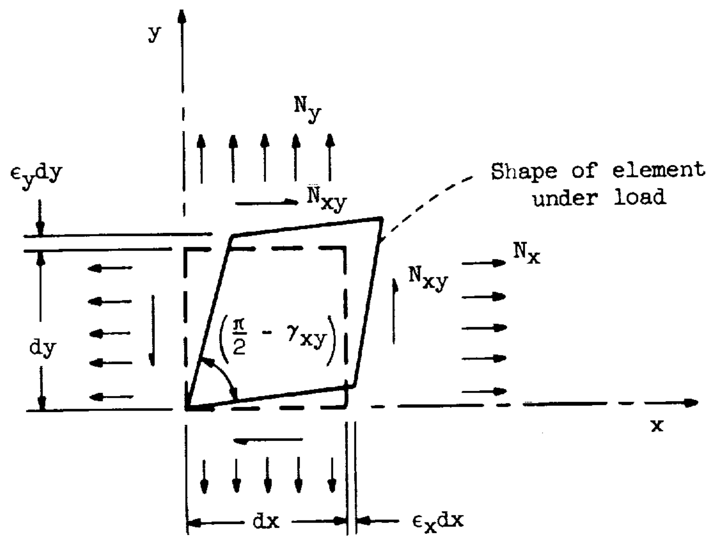

Figure 1.- In-plane loadings and deformations of shell element:
Extension and shear.

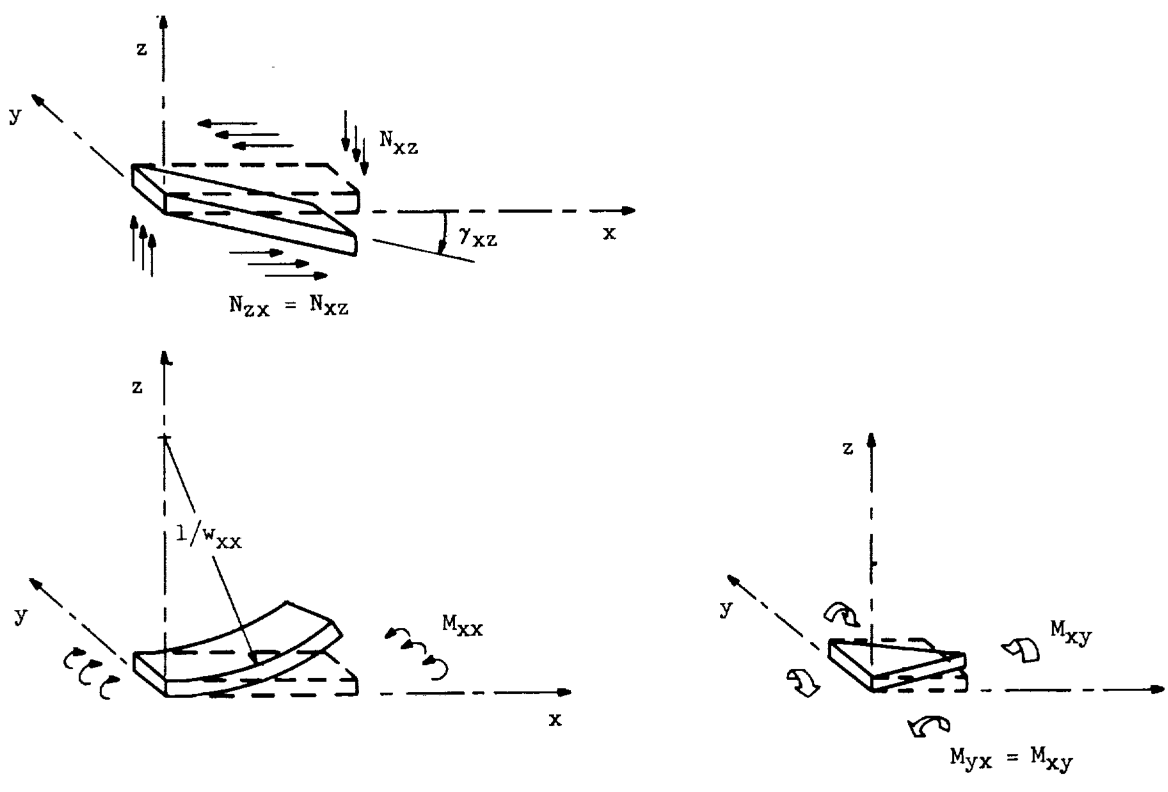

Figure 2.- Transverse loadings and deformations of shell element:
Beam shear, bending, and twisting.

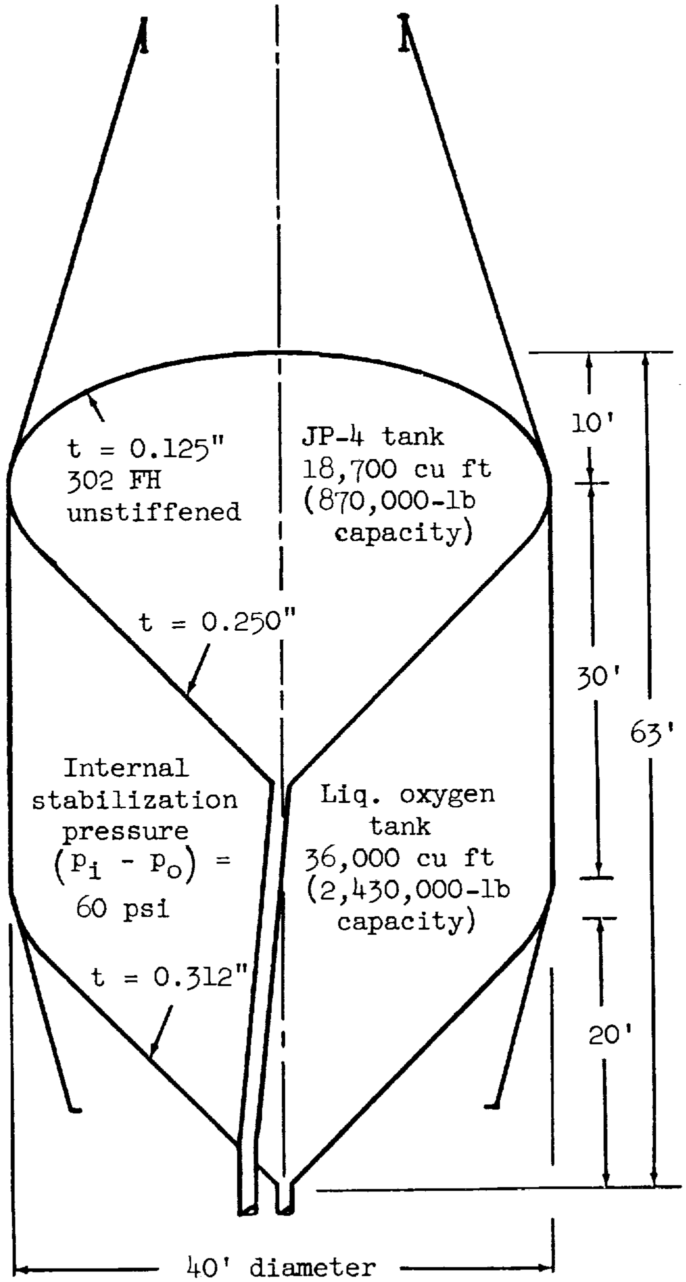

Figure 3.- Assumed tank structure for model test study.

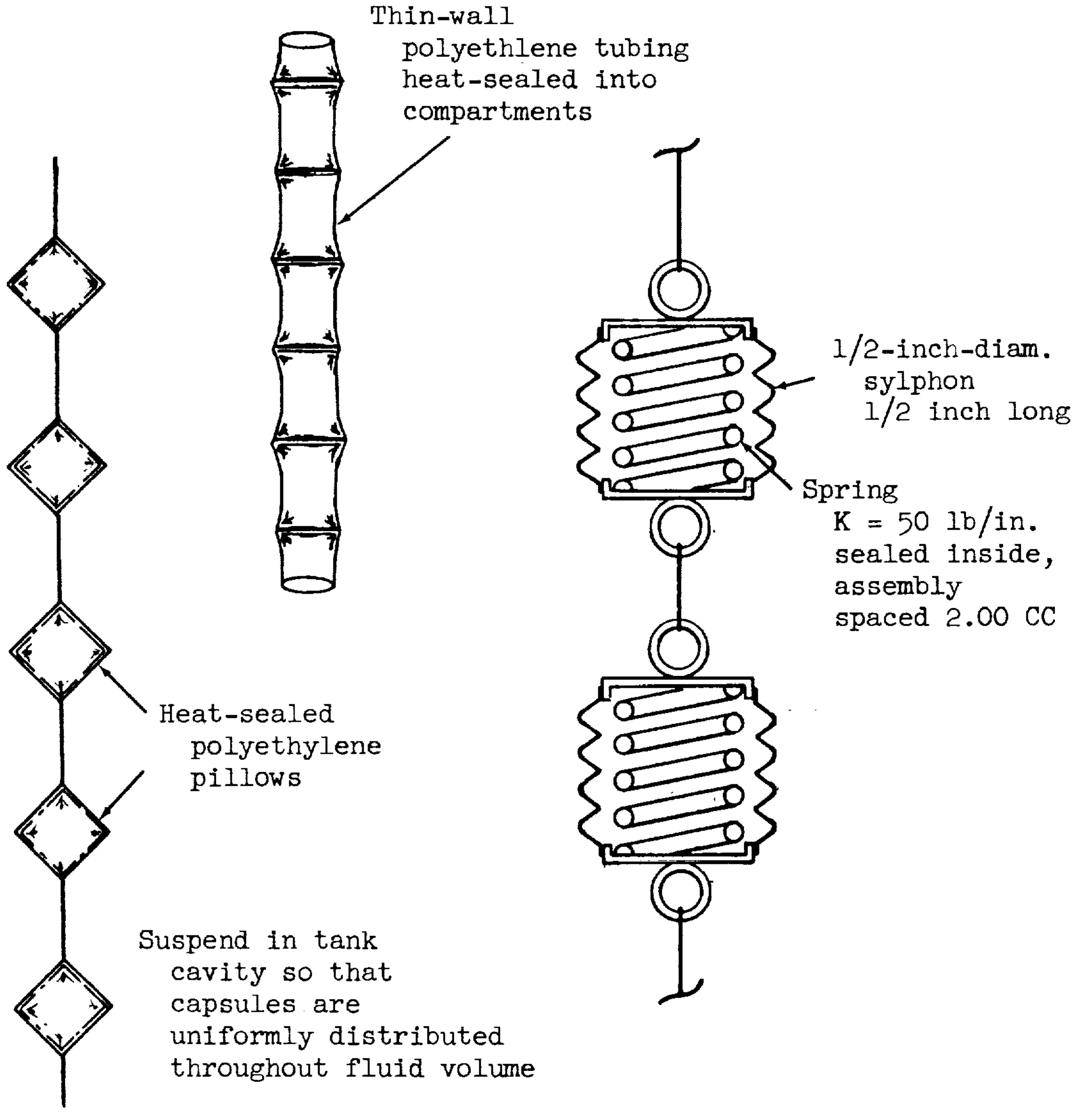

$$\beta_{total} = \beta_{fluid} + \beta_{add}$$

$$\beta_{add} = N \frac{A^2}{k} 2120 \text{ per atmosphere}$$

N = number of capsules used per cu ft of fluid
A = effective cross-sectional area of sylphon, ft^2
k = spring constant, lb/ft

Figure 4.- Methods of artificially increasing compressibility.